Extended Abstracts of the 2011 International Conference on Solid State Devices and Materials, Nagoya, 2011, pp90-91

Impact of Interface State Density on MOSFET Local Oxide Capacitance Degradation During Hot-Carrier Stress

Ivan Starkov* and Hajdin Ceric
Christian Doppler Laboratory for Reliability Issues in Microelectronics at the
Institute for Microelectronics, TU Wien, Gußhausstraße 27-29, A-1040 Vienna, Austria
*corresponding author: Phone: +43-1-58801-36035, E-mail: starkov@iue.tuwien.ac.at

1. Introduction

Basic methods for extraction of the lateral interface state density profile $N_{\rm it}(x)$ from charge-pumping data employ the oxide capacitance $C_{\rm ox}$ [1–3] as a crucial parameter. Although Lee *et al.* [2] claimed that the coordinate dependence of the capacitance $C_{\rm ox}(x)$ should be respected, usually $C_{\rm ox}$ is treated as a constant parameter of the device [3]:

$$C_{\rm ox} = \varepsilon_{\rm ox}/t_{\rm ox}. \qquad (1)$$

where $t_{\rm ox}$ is the oxide thickness at the center of the device and $\varepsilon_{\rm ox}$ is the dielectric permittivity. In a series of works [2] it is possible to find extension of the eq.(1) when $t_{\rm ox}$ depends on x ($t_{\rm ox} = t_{\rm ox}(x)$). In fact, in such an approach the capacitor is considered ideal or, in other words, the electric field is assumed uniform. In practice, however, a substantial distortion occurs near the source/drain ends of the gate. The aforementioned simplification does not strongly affect the transistor characteristics. However, the electric field non-uniformity is of special importance for the extraction of the interface state density profile after hot-carrier stress because the $N_{\rm it}(x)$ peak is located near the drain end of the gate [4] where the capacitor non-ideality is most pronounced.

In this work we refine a technique for the extraction of the $N_{\rm it}$ profile from charge-pumping data described in [1] by considering the dependence of the oxide capacitance on the lateral coordinate more accurately. First, interface state build-up affects $C_{\rm ox}$ and thus the extraction routine has to be performed self-consistently. Further, we consider the effect of the oxide field non-uniformity on the oxide capacitance. Additionally, geometrical peculiarities of the device are also taken into account. Finally we summarize the impact of the various factors on accuracy of the extraction.

2. Local Oxide Capacitance

For our investigation we use an n-channel MOSFET with a channel length of 0.25μm (sketched in Fig. 1). All lateral coordinates x refer to an origin at the left edge of the source contact. The device was stressed at a gate voltage of $V_{\rm gs} = 2.0$V and a drain voltage $V_{\rm ds} = 5.0$V at the ambient temperature of $T = 25^{\rm o}$C.

For consideration of the local oxide capacitance we use the method developed by Lee *et al.* [2]. The presence of a probe oxide charge ($Q_{\rm ot}$) leads to a local threshold voltage $V_{\rm th}(x)$ [1] shift and the oxide capacitance is thus found as:

$$C_{\rm ox}(x) = -Q_{\rm ot}/\Delta V_{\rm th}(x). \qquad (2)$$

The profile $C_{\rm ox}(x)$ is then used to extract the $N_{\rm it}(x)$ distribution from [1,3]:

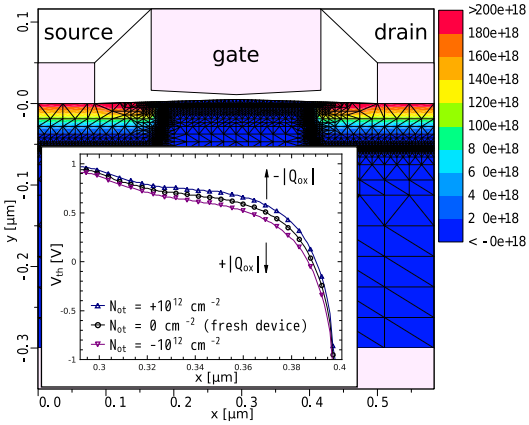

Fig. 1: The architecture of the device subjected to hot-carrier stress. The donor doping profile is represented by the color scheme. Inset: local threshold voltage distributions with uniform oxide charge profiles.

$$V_{\rm th,stress}(x) = V_{\rm th}(x) - \frac{q\Delta N_{\rm ot}(x)}{C_{\rm ox}(x)} + \frac{q\Delta N_{\rm it}(x)}{2C_{\rm ox}(x)}, \qquad (3)$$

where $\Delta N_{\rm it}(x)$ and $\Delta N_{\rm ot}(x)$ is the change between pre- and post-stress concentrations of interface traps and bulk oxide charges.

The extraction procedure includes, therefore, the following steps as an addition to the extraction technique described in [1]. Using the device and circuit simulator MINIMOS-NT [5] we introduce an artificial uniform bulk oxide charge into the transistor and calculate the threshold voltage shift. A typical example of the $V_{\rm th}(x)$ shift induced by a uniform oxide charge density of $\pm 10^{12}$cm^{-2} is shown in Fig. 1 inset. Then we calculate $C_{\rm ox}(x)$ according to eq.(2). This procedure is performed at each stress time step considering the corresponding $N_{\rm it}(x)$ profile in all simulations. In other words, the impact of interface state density (generated during the stress) on the local capacitance is considered. Then, using this calculated $C_{\rm ox}(x)$ and employing formula eq.(3), we extract the interface state density for the next time step.

This method is developed to be applied to devices which have complicated doping profiles in the substrate (see Fig. 1). As a consequence, one can imagine that the capacitance may be affected by the presence of these doping concentrations. To check this, we used an artificial capacitor with the same dielectric film (i.e. with same geometrical features) as in the transistor under test. In this case we calculated the capacitance as ratio between the interface charge and the difference in the electrical potential and compared it to that obtained according to eq.(2).

Fig. 2 demonstrates that the substrate doping does not affect the capacitance of the oxide film. At the same time, the expression eq.(1) corrected for $t_{ox} = t_{ox}(x)$ leads to a substantially different results. The most pronounced peculiarity is observed at $x \sim 0.42\mu$m, i.e. just near the drain side of the gate where the abrupt change in the oxide thickness occurs (see Fig. 2, inset). Note that such an abrupt reduction in $C_{ox}(x)$ is unphysical and eq.(1) should not be used.

3. Results and Discussion

To extract the density of interface states we employed the procedure described in the previous section incorporated into the scheme described in [1]. Fig. 3 demonstrates the dependence of the oxide capacitance on the lateral coordinate extracted for several time steps. This graph depicts that the change of C_{ox} grows with the stress time. In other words, higher $N_{it}(x)$ induces a stronger change in the capacitance. One can see that in the vicinity of the drain edge of the gate the difference may reach $\sim 30\%$ of the initial value. This is related to the superposition of two factors. First, the N_{it} profile peaks just in this area and the interface state impact on C_{ox} is most significant at this position. Second, at the end of the gate the capacitor electric field most severely deviates from the uniform case, thereby producing distortion in $C_{ox}(x)$.

In Fig. 4 the $N_{it}(x)$ profile extracted with and without capacitance corrections are shown. The most significant discrepancy in $N_{it}(x)$ is also observed near the drain region of the device, which correlates with the findings from Fig. 3. It is worth emphasizing that already at 10^3s the difference in N_{it} reaches $\sim 15\%$. The spurious result produced with the model ignoring the $C_{ox}(x)$ change may lead to an ambiguous picture of hot-carrier induced degradation. This behavior is easily understood assuming that during the stress generated interface states act as an additional series capacitance connected to the C_{ox} of the "virgin" device. Hence, the total capacitance of the system is decreased, which affects the electrostatics of the transistor, in particular the threshold voltage profiles (see Fig. 4, inset).

4. Conclusion

We have demonstrated the effect of the interface states build-up on the local oxide capacitance. The presence of $N_{it}(x)$ may change $C_{ox}(x)$ by 30% already at 10^3s. Therefore, the change of the capacitance should be taken into account while extracting the interface state density from charge-pumping data. The model also considers the variation in the oxide thickness with the coordinate and the non-uniformity in the capacitor electric field. Finally, we have shown that $N_{it}(x)$ profiles obtained with respect to the aforementioned features and without corresponding corrections are different.

References

[1] W. K. Chim, S. E. Leang, and D. S. H. Chan, J. Appl. Phys., **81** (1997) 1992.

[2] R. G.-H. Lee, J.-S. Su, and S. S. Chung, IEEE Trans. Electron Dev., **43** (1996) 81.

[3] S. Mahapatra, D. Parikh, V. Rao, C. Viswanathan, and J. Vasi, IEEE Trans. Electron Dev., **47** (2000) 171.

[4] A. Bravaix and V. Huard, in *Proc. European Symposium on Reliability of Electron Devices Failure Physics and Analysis (ESREF), tutorial*, 2010.

[5] Institute for Microelectronic, TU Wien, *MiniMOS-NT Device and Circuit Simulator*.

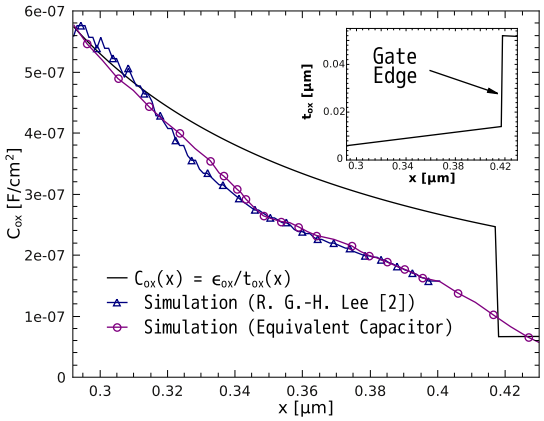

Fig. 2: The local oxide capacitance calculated within the approach [2] and compared with the capacitance of the dielectric film of the same geometry as that employed in the transistor under test. For comparison the $C_{ox}(x)$ calculated with eq.(1) corrected for $t_{ox} = t_{ox}(x)$ is also plotted. Inset: the dependence of the oxide thickness vs. the lateral coordinate.

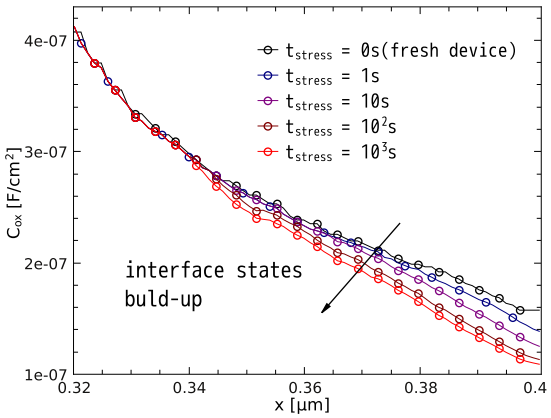

Fig. 3: Local oxide capacitance degradation due to the hot-carrier stress.

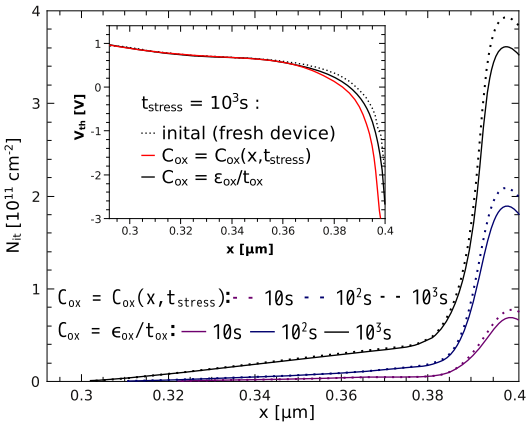

Fig. 4: The interface states profile evolution with (dashed lines) and without account of local oxide capacitance degradation. Inset: local threshold voltages corresponding to obtained $N_{it}(x)$ profiles.